AD-A108 152 CALIFORNIA UNIV SAN DIEGO LA JOLLA DEPT OF ELECTRICA--ETC F/G 3/2
THE THREE-DIMENSIONAL STRUCTURE OF THE SOLAR WIND FROM RADIO SC--ETC(U)
APR 81 B V JACKSON, A NAGENDRAN F19628-77-C-0161

UNCLASSIFIED AFGL-TR-81-0039 NL

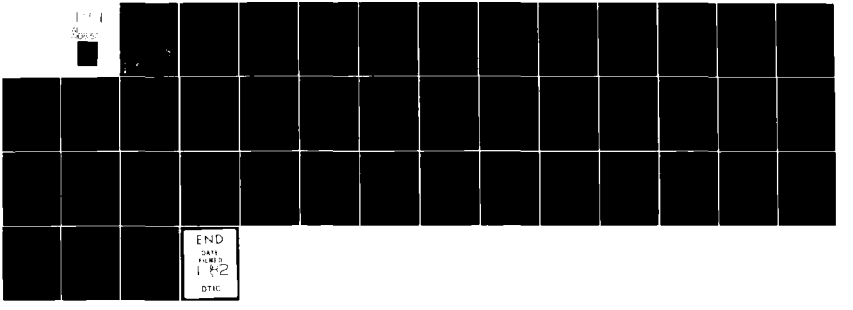

END
DATE FILMED
1 82
DTIC

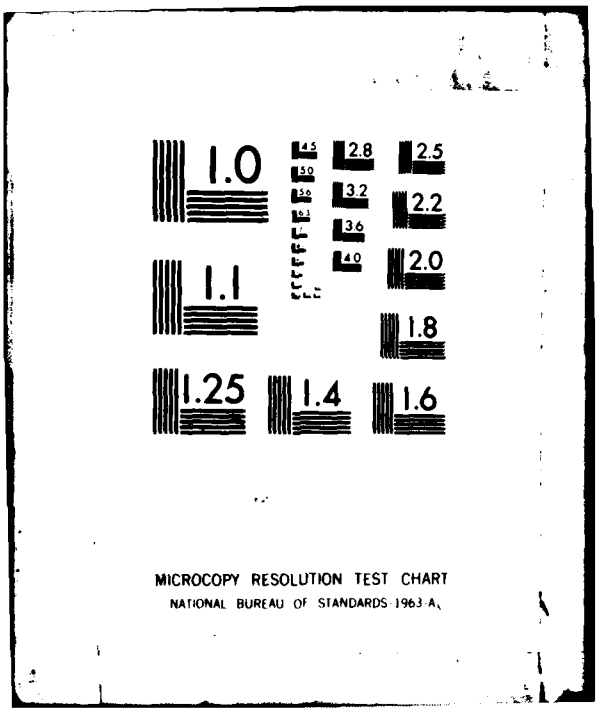
1.0
1.1
1.25
1.4
1.6
1.8
2.0
2.2
2.5
2.8
3.2
3.6
4.0
4.5
5.0
5.6
6.3
MICROCOPY RESOLUTION TEST CHART
NATIONAL BUREAU OF STANDARDS 1963-A

Unclassified

SECURITY CLASSIFICATION OF THIS PAGE (When Data Entered)

REPORT DOCUMENTATION PAGE		READ INSTRUCTIONS BEFORE COMPLETING FORM
1. REPORT NUMBER AFGL-TR-81-0039	2. GOVT ACCESSION NO. AD-A108152	3. RECIPIENT'S CATALOG NUMBER
4. TITLE (and Subtitle) THE THREE-DIMENSIONAL STRUCTURE OF THE SOLAR WIND FROM RADIO SCINTILLATIONS		5. TYPE OF REPORT & PERIOD COVERED Final Report 25 Feb 1977 - 30 Sept 1981
		6. PERFORMING ORG. REPORT NUMBER
7. AUTHOR(s) B. V. Jackson A. Nagendran		8. CONTRACT OR GRANT NUMBER(s) F 19628-77-C-0161
9. PERFORMING ORGANIZATION NAME AND ADDRESS Dept. of Electrical Engineering & Computer Sciences University of California, San Diego La Jolla, California 92093		10. PROGRAM ELEMENT, PROJECT, TASK AREA & WORK UNIT NUMBERS 61102F 2311G3AD
11. CONTROLLING OFFICE NAME AND ADDRESS Air Force Geophysics Laboratory Hanscom AFB, Massachusetts 01731 Monitor/Richard C. Altrock/PHS		12. REPORT DATE April 1981 13. NUMBER OF PAGES 44
14. MONITORING AGENCY NAME & ADDRESS(if different from Controlling Office)		15. SECURITY CLASS. (of this report) Unclassified 15a. DECLASSIFICATION/DOWNGRADING SCHEDULE

16. DISTRIBUTION STATEMENT (of this Report)

Approved for public release; distribution unlimited

17. DISTRIBUTION STATEMENT (of the abstract entered in Block 20, if different from Report)

18. SUPPLEMENTARY NOTES

19. KEY WORDS (Continue on reverse side if necessary and identify by block number)

Solar corona
Solar wind
Solar radio observations

A

20. ABSTRACT (Continue on reverse side if necessary and identify by block number)

In the followino report we present two papers pertinent to a portion of of the work done for contract F19628-77-C-0161. First we report on IPS transients that are associated with large solar flares. Second, we report on progress to upgrade the UCSD telescope system to better understand these solar wind features.

DD FORM 1 JAN 73 1473 EDITION OF 1 NOV 65 IS OBSOLETE

Unclassified

SECURITY CLASSIFICATION OF THIS PAGE (When Data Entered)

Preface

Since 1972 the UCSD 74 MHz radio observatory has continuously monitored the solar wind using the method of interplanetary scintillation (IPS). The two reports presented here bear on the problems involved in tracing the fast changing three dimensional structure of the solar wind from the solar surface out to the vicinity of the earth.

The interplanetary scintillation technique is a radio propagation method for studying the velocity and small scale (~100 - 1000 km) turbulence in the solar wind. The signals are cross-correlated from three spaced antennas to yield time offsets from which the speed of the scintillation pattern can be deduced. Comparisons of IPS observations with spacecraft measurements have shown excellent agreement when the IPS source lies in the ecliptic plane. Since our equipment relies on the use of natural radio sources, we are not restricted to observations in the ecliptic. Furthermore, observations can be made in the direction of many radio sources (almost) simultaneously so as to generate a three-dimensional map of the solar wind. .

The eight-year data base is important for correlative studies throughout the solar cycle. In our analysis we emphasize three time scales - a) the solar cycle evolution of six month average velocity structures b) studies of one solar rotation duration c) variations in the solar wind structure on time scales of a few days. In the past we have placed more emphasis on the first two time scales. Only recently have we increased our spatial coverage by observing double the number of sources per day as during the period 1972-79. Daily variations in solar wind structures are best observed with high spatial resolution.

This report consists of two parts that concentrate on our ability to obtain data and observe variations on the shortest time scale. Other work completed during the period is contained in Scientific Reports 3b and 3c. In particular we first

report on transients in the solar wind associated with solar flares. This study covers the time period between 1972 and 1979 and serves as a basis for future studies of individual events - studies that will now be more conclusive because of our increased time and spatial coverage. The second report details the observations of new sources measured by the UCSD telescopes. Not only do these new sources help in short term transient studies, but they also help determine how much bigger arrays would be necessary to increase spatial coverage by orders of magnitude and thus obtain better data during rapidly changing events.

Contents

FLARE RELATED TRANSIENTS IN THE SOLAR WIND AS INFERRED FROM IPS OBSERVATIONS AT UCSD

A. NAGENDRAN

DEPARTMENT OF ELECTRICAL ENGINEERING AND COMPUTER SCIENCES
UNIVERSITY OF CALIFORNIA, SAN DIEGO
LA JOLLA, CALIFORNIA 92093

ABSTRACT

A study is made of solar wind disturbances detected by IPS observations, and their relationship to H-α flares. At least two thirds of the most energetic flares (area x brightness x duration) caused detectable disturbances. The rate of such associations did not vary significantly over the solar cycle. One particular event, March 6th 1978, was studied in detail; it showed a much greater velocity increase near the flare normal N28^{o} than at the earth at S7^{o}. Six outbursts from a particular long-lived active region were also studied from March-July 1978; in each case a solar wind disturbance was evident near the flare normal.

Flare Related Transients in the Solar Wind as Inferred from IPS Observations at UCSD

INTRODUCTION

The IPS method [1, 2, 3] uses three spaced antennas to record signals from a small diameter radio source. The scintillations in the intensity of the signals at each antenna are caused by inhomogeneities in the solar wind; the signals are cross-correlated to yield time offsets, from which the speed of the scintillation pattern can be deduced. Solar wind speeds measured by IPS at UCSD have been calibrated with spacecraft observations [4] and found to be within $\pm$ 50 km/sec of the solar wind speed at the point where the radio-wave scattering is the strongest. This point on the line of sight to the radio source is referred to as the "sub-scattering point". Two velocity estimates are made from the cross-correlation functions of the signal between any pair of antennas. The first uses the time offset of the midpoint of the cross-correlation function, while the second uses the time offset of the peak of the cross-correlation function. These two velocity estimates are referred to as "V_{mid}" and "V_{pk}" respectively.

IPS measurements of the solar wind velocity have been used to study the association between co-rotating high speed streams and coronal holes [5, 6, 7]. They have also been used to study the high speed polar solar wind and its evolution with the solar cycle [8, 9].

Flares are sudden, localized brightenings which can be observed in H-α. The intensity rises to a maximum in a few minutes, followed by a decay period which may last from tens of minutes to a few hours. They occur in regions of strong magnetic fields of the order of 10^2-10^3 gauss. Their magnitudes are estimated on a scale of importance 1-, 1, 2, 3 and 4, mainly based on area, corrected for foreshortening of the disk. The area (in 10^{-6} of the visible

hemisphere) for the above mentioned scale is < 100, 100-250, 250-600, 600-1200, and > 1200 respectively [10].

The effects of solar flares on the interplanetary medium have been studied by associations with geomagnetic observations, spacecraft observations, and IPS observations. Hundhausen [11] summarizes the spacecraft observations of interplanetary shock waves. From a sample of 27 shocks he obtains a mean speed of 500 km/sec for the shock wave (at 1 AU) and a mean propagation speed of 730 km/sec. He concludes that deceleration of shock waves would be common, although some events are presented where there was no deceleration.

Rickett [12] presents IPS observations of solar wind disturbances following the flares of August 2, 4 and 7, 1972. By comparing IPS, spacecraft, and geomagnetic observations he concludes that the extent of the disturbance front at 1 AU covered about $\pm$ 60° in longitude and more than 30° in latitude from the flare normal.

Theoretical calculations of shock waves have been carried out by De Young and Hundhausen [13]. They have obtained numerical solutions for two-dimensional, time dependent hydrodynamic flow (ignoring magnetic fields) in spherical coordinates. They calculate the disturbance shapes and transit times to 1 AU of a blast wave. The dependence on initial disturbance energy and angular extent is examined.

Rust et al [14] have done numerical simulations of coronal transients using two-dimensional magnetohydrodynamic models with adjustable initial temperature and density perturbations and almost arbitrarily selectable initial conditions. They consider the effects of magnetic topology and the magnitude and duration of the driving pulse. They conclude that although a mass ejection may be driven by a pressure pulse at its base, the (stationary) magnetic field guides and constrains the outward motion of the coronal plasma. As an alternative to a pressure pulse, they suggest that (changing) magnetic fields could be forcing

the motion of the ejecta in ways that have not been modeled.

In this report, we describe the results of a study of H-α flares and related solar wind disturbances as observed by IPS for the period 1972-1979. We conclude that only the most energetic (area x brightness x duration) solar flares are associated with detectable changes in the solar wind.

In section 1 we describe details of the data scan, the results of which are summarized in Tables 1.1, 1.2 and 1.3.

In section 2 we describe in some detail the response of the solar wind to a particular event of March 06, 1978. An interesting conclusion for this event is that the propagation of the flare associated disturbance was not spherically symmetric with respect to velocity and deceleration.

In section 3 we present a sequence of six large flares which occurred in the same active region over a period of six solar rotations. For each event we had a favorably situated radio source to make IPS observations. For each event we find that the ambient solar wind speed increased by a factor of approximately 2.

1. Solar cycle variation of large H-α flares and related IPS velocity changes

All flares of brightness B, duration $\geq$ 60 minutes, and area $\geq$ 1 for April 1972-December 1979 have been selected from SGD parts I and II. For each of these flares the IPS velocity (V_{mid}) for that day and following 1-3 days have been scanned for a velocity increase of $\geq$ 100 km/s. (On the whole, the velocity increase is seen on a source which is close to the flare normal).

In the cases where large flares occur closely spaced (in time), there may be several peaks in the IPS velocity series. In this case, the association between each flare and corresponding IPS velocity increase has been made by

rejecting those candidates which imply an average speed of propagation from the sun to the subscattering point of $\leq$ 500 km/s or $\geq$ 2000 km/s. We have rejected average speeds less than 500 km/sec, in order to resolve unambiguously the (H-α flare) - (IPS velocity increase) associations. This seems justified because we have observations suggesting that the largest, longest duration flares were indeed associated with sudden, high speeds in the solar wind. We also reject associations which imply average speeds greater than 2000 km/sec; this is a reasonable upper bound, since we know from coronal transient observations that mass ejections from the corona do not travel faster than $\approx$ 2000 km/sec.

Continuous IPS data was not available for us to analyze each of the big flares during 1972-1979. There are two reasons for this. Firstly, some of the big flares occurred when the IPS radio sources were unfavorably situated w.r.t. the flare normal. Secondly, when a large active region on the sun crosses the central meridian plane, the UCSD observing system is swamped by solar radio noise for most sources having elongations $< 90°$.

For those flares for which continuous IPS data was available, a decision was made whether the flare was/was not associated with a velocity increase of $\geq$ 100 km/sec in the solar wind, as observed on a source whose subscattering point was within 60° of the flare normal. Thus, for each big flare during 1972-1979, we look at the IPS velocity series and make a 3-way decision, namely: a flare 1) was 2) was not associated with a velocity increase, or 3) there was insufficient data.

Using the above scanning technique, Tables 1.1, 1.2 and 1.3 have been compiled. These tables are an attempt to display the variation over one solar cycle, and to display the variation with size (area) and duration of the H-α flare.

The conclusion here is that large solar flares are associated with velocity increases in the solar wind. Also, the IPS method allows us to observe disturbances which propagate away from the earth, which would be unnoticed by earth orbiting spacecraft. In order to better understand the detailed morphology of the disturbance propagation, we intend to model the IPS parameters for radio scintillations due to a solar wind disturbance.

Figure 1.1 (a, b, c) is a set of three histograms for each category of H-α flares in Tables 1.1, 1.2 and 1.3. The solid line is the number of flares in that category. The broken line is the number of associated IPS velocity increases.

Some interesting features of Tables 1.1-1.3 are: 1) IPS velocity response appears sensitive to the flare area (from 1B to 2B) and duration. However, the area measurement is subjective, and the only firm conclusion is that very large flares (area $\geq$ 2) of brightness B, and long duration ($\geq$ 120 minutes) are associated with high speeds in the solar wind lasting for at least 24 hours.

(It is more difficult to investigate the sensitivity to the flare duration, which in this study varied from 60 min-600 min.).

2) There were more flares of area $\geq$ 2 during 1978 than in 1979, although general solar activity was increasing. This is interesting because it may be related with the "closing up" of polar coronal holes and the attendant disappearance of the high speed polar solar wind in 1978 [Coles et al., 1980].

[Appendix is a detailed list of major solar flares for April 1972-December 1979, with dates, area x brightness, duration (in minutes), location on solar disk, and the three-way decision w.r.t. IPS velocity increase. Flares which occurred closely spaced in time have been grouped together with the comment "resolution" - meaning that it was not possible to unambiguously associate the single IPS velocity increase with the several events in the group].

2. Flare of March 06, 1978 and associated solar wind response

Major flares (importance $\geq$ 1B and duration $\geq$ 40 min) for March 1978 (from SGD):

March 03	1B	55 min	S27 W05
04	1B	120 min	N15 E45
06	2B	166 min	N28 E22
11	1B	41 min	N24 W38
13	1B	56 min	N25 W76
15	1B	40 min	N19 E65

The following discussion makes implicit references to Figures 2.1, 2.2 and 2.3. Figure 2.1 is a graph of daily IPS observations of solar wind velocity for the period March 06-10, 1978. The circles refer to the V_{mid} velocity and the crosses refer to the V_{pk} velocity. The "3C" radio source on which scintillations were observed is also noted. (JAP) refers to IPS observations made at the Research Institute of Atmospherics, Nagoya University. Also graphed (broken line) is the solar wind velocity (3 hour averages) measured by earth orbiting spacecraft IMP 7 and 8. The hatched histogram at the bottom is the K_p index (3 hour averages) from SGD. Finally, the H-α flare of March 06 is denoted by an arrow, and a hatched area representing its duration.

Figure 2.2 is an ecliptic projection of the UCSD observing system. It indicates the relative positions of the eight radio sources, the sun, and the earth for any day of the year. The position of the sun and the direction of the flare normal for the March 06 event are noted. Also marked are the heliographic latitudes of the earth (- 7°) and the subscattering point of 3C48 (+ 12°).

IPS velocity observations of 3C48 show a sudden increase from $\leq$ 450 km/s on the preceding six days to a velocity of 830 km/s on day 66 (V_{mid} and V_{pk} are within 50 km/s of each other, except on day 65 when the values are 434, 554 km/s respectively). On day 67 the data was poor (edit = 1) and is unreliable.

Japanese IPS observations show the velocity observed from 3C48 dropping to 640 km/s six hours after the UCSD observation of 830 km/s. On the following days, both UCSD and Japanese data show that the velocity remains high ($\geq$ 500 km/s) for days 67, 68, 69. Subsequently, it tails off to a value of 355 km/s on day 72. (Except for day 67, the IPS data on 3C48 is very good).

Observations of other sources 3C144, 3C147, 3C161 shows velocities of $\simeq$ 350 km/s on days 65, 66 and 67. Unfortunately, there is no data for these sources on day 68. However, Japanese observations show a velocity of 300 km/s on day 68 for 3C144, and UCSD observations show velocities $\simeq$ 300 km/s for 3C144 on days 69 and 70. (V_{pk} is within $\pm$ 50 km/s of V_{mid}, except on day 69), 3C161 shows 300 km/s ($\pm$ 50 km/s) on days 69 through 73. V_{pk} does not deviate from V_{mid} by more than 50 km/s on these days. The velocities observed on 3C147 also lie close to those observed on 3C144 and 3C161, although there was no data for this source on day 69 as well as 68.

From the geometry of the sources 3C48, 3C144, 3C161 (and 3C147) we conclude that the high speed seen on 3C48 occurred within a narrow region of the solar wind. It is also interesting to note that the velocity observed on source 3C298 (which is in a direction opposite to 3C48) increases from 335,327 km/s (V_{mid}, V_{pk}) on day 65, to 639,696 km/s (V_{mid}, V_{pk}) on day 67. There was no data for 3C298 on day 66.

Since the lines of sight of both 3C48 and 3C298 are inclined north of the ecliptic by $\simeq$ 20°, it appears that high speed ejecta from the flare was directed in a north westerly direction from the flare site (w.r.t. sun).

Geomagnetic and spacecraft data suggest that there was a slight disturbance close to earth as a result of the flare of March 06. The K_p index (from SGD) increased on day 67 to a value of 5- for the 3 hour period starting at 1200 UT. The K_p index was $\leq$ 3 during the preceding 48 hours.

K_p index (3 hours avgs) from SGD:

March 08: 1+, 1-, 1+, 1+, 5-, 3+, 5+, 4 (day 67)

March 09: 3-, 3+, 3-, 3+, 2+, 2+, 3+, 3- (day 68)

The Boulder geomagnetic substorm log reported a global disturbance commencing at 1440 UT and lasting until 2200 UT. Thus we estimate the duration of the disturbance at earth to be $\simeq$ seven hours. (From the K_p index change we would estimate it to be $\simeq$ 12 hours.)

Spacecraft data close to earth:

Spacecraft data (IMP 7 and 8) show a gradual velocity increase in the solar wind close to earth starting at 350 km/s on day 67 and reaching 500 km/s on day 68. The velocity falls off sharply to 400 km/s on day 69, after which there are some data gaps. Spacecraft data also indicate a particle density increase from 10 cm^{-3} to 40 cm^{-3} commencing on day 67 at $\simeq$ 1200 UT and lasting $\simeq$ 12 hours. This agrees rather well with the geomagnetic disturbance commencement and duration. Solar wind temperature measurements from IMP 8 show a gradual increase in the thermal speed starting at 40 km/s on day 67 (1200 UT) and reaching 75 km/s approximately 12 hours later.

Shape and deceleration of the disturbance:

We can now compare observed and average velocities of propagation of the disturbance at two points in the solar wind. One is close to earth and the other is north of the ecliptic and makes a 17° angle (earth-sun-scattering point) in the ecliptic plane.

Max velocity from 3C48 = 830 km/s.

Max velocity from earth orbiting spacecraft = 500 km/s.

The subscattering point of 3C48 was 0.8 AU from the sun. Thus we see that there is a considerable difference in the velocities at $\simeq$ 1 AU.

Avg velocity from 3C48 velocity increase = 908, 2802 km/s (min, max).

Avg velocity from K_p index increase = 840 km/s.

Comparing the average and observed values for the case of 3C48 and earth, we see that there was little or no deceleration for 3C48, while there was considerable deceleration in the direction of the earth. This is interesting because the subscattering point of 3C48 was N19° E17° of the earth (in a heliographic coordinate system), while the flare normal was N28° E22°.

CONCLUSIONS

(a) IPS observations of 3C48 indicate that the propagation of ejecta from the 2B flare of March 06, 1978 was not spherically symmetric w.r.t. velocity and deceleration. At 1 AU, we have observed a speed 830 km/sec close to the flare normal, and a speed of 500 km/sec away from the flare normal.

(b) The fact that the velocity remained high ($\geq$ 500 km/s) for 4 days in the direction of sun - 3C48 scattering point suggests the temporary formation of a small, high speed emitting region on the sun.

3. IPS observations of solar wind response to a flaring active region (March-July 1978)

In this section we present observations of six large H-α flares which occurred close to a single site on the solar surface, and located within a large northerly active region which survived intact during the period March-July 1978. The data has been organized into 4 tables (Tables 3.1-3.4), where each table presents some aspect of the H-α flares and the solar wind response to all six flares. The objective here is to derive a general observational result for the solar wind response to the most energetic solar flares.

Figure 3.1 is an ecliptic projection of the UCSD observing system, with the positions of the sun and directions of the flare normal for the six H-α flares.

Table 3.1 displays the dates and position on disk of the flares under investigation. The time period March 06-July 09 covers approximately six solar rotations. Column 3 of Table 3.1 displays the position of each flare mapped to an arbitrary rotation number frame. This shows that the events of March 06, April 28, May 31, and June 22 occurred within an area covering 20° of longitude and 10° of latitude on the solar disk. The McMath-Hulbert calcium report (SGD) shows that the flare sites for these events falls squarely within the boundary of a long-lived calcium plage region. A detailed study of the origin and evolution of this active region is not being attempted here. Column 4 of Table 3.1 indicates the presence or absence of type II and type IV radio bursts which occurred simultaneously with the flare. Speeds of the moving radio bursts are not available.

Table 3.2 displays geomagnetic disturbance data following the flares of March 06-July 09. In columns 3 and 4 we attempt to correlate the duration of the flare with the duration of the K_p index increase. Column 5 displays the average speed of propagation of the disturbance toward earth, calculated from the time lag. Note that the flares of April 13 and July 09 had flare normals 85° and 70° away from the earth, and did not produce geomagnetic disturbances.

Table 3.3 displays the IPS velocity response associated with the six flares. The V_{mid} velocity of the source whose subscattering point was closest to the flare normal has been tabulated for the day before and after the velocity increase (day numbers in parentheses). The source for which the velocity increase was seen is identified in column 5, while the angular displacement of the flare normal and subscattering point (in the ecliptic) is in column 4. We see that the solar wind velocity increases by a factor of $\sim$ 2 for these events.

Table 3.4 summarizes the observed and average velocity of propagation of the flare associated disturbances as derived from IPS and K_p index measurements. Column 1 lists the observed IPS V_{mid} and V_{peak} on the day of onset of the velocity increase (the radio source is in parentheses). We see that for the events of March 06, April 28 and July 09, the V_{mid} and V_{peak} velocities are within $\pm$ 25 km/s of each other. For the event of April 13 the V_{peak} exceeds V_{mid} by 86 km/sec, while for the events of April 28 and June 22 the V_{peak} is less than V_{mid} by 55 and 68 km/sec respectively.

Column 2 of Table 3.4 lists the average velocity of propagation between the flare and the subscattering point (of the radio source in question). This is calculated from the distance (in column 4) and the time lag to the IPS velocity increase. Since the time lag could be overestimated by up to 24 hours, we calculate a minimum and a maximum for the IPS average. The true average must lie between the IPS minimum and maximum. For the events of May 31 and June 22 we see that the average velocity of propagation from K_p index (column 5) lies between the IPS minimum and maximum, while for the events of March 06 and April 28 the K_p average is less than the IPS minimum average by 68 km/sec and 73 km/sec respectively. For the events of April 13 and July 09 there were no geomagnetic disturbances, as already mentioned w.r.t Table 3.2.

We can use Table 3.4 to identify events where there was deceleration of the flare associated disturbance. If the IPS "observed" velocity (V_{mid}) was lower than the IPS "minimum average" velocity, then we conclude that there was deceleration.

Thus we see that there was deceleration for the event of April 28, the velocity difference being 310 km/sec. If the IPS "observed" velocity lies between the IPS "minimum average" and the "maximum average" velocities, then the event is consistent with no deceleration, although there may have been some deceleration. We do not consider the case of acceleration, because we have used the implication of acceleration to reject flare-IPS velocity associations!

We do not consider the case of acceleration, because we have used the implication of acceleration to reject flare-IPS velocity associations!

Summary and Discussion of Section 3

We have presented IPS and K_p index data on six large flares which occurred within (or close to) a large, long-lived (6 rotations) active region. In section 2 we saw that the flare induced disturbance of March 06, 1978 was not spherically symmetric. Thus we have confined ourselves here to IPS observations of radio sources "close" to the flare normal. We find that the ambient solar wind speed increases by a factor of ≈ 2 for each of these events (average: 371-707 km/sec).

We have detected deceleration of the disturbance using estimates of the average speeds from the time lag to IPS and K_p index observations. Some points worth noting are:-

(a) Attempts to compare average speeds from IPS and K_p index must take into account the angular separation of the radio source subscattering point and earth, since we cannot assume spherical symmetry of the disturbance.

(b) Deceleration of the disturbance may depend on distance from the sun, as well as angular displacement from the flare normal.

REFERENCES

1. Dennison, P. A. and Hewish, A., The solar wind outside the plane of the ecliptic, Nature 213, 343-346 (1967).
2. Armstrong, J. W. and Coles, W. A., Analysis of three-station interplanetary scintillation, J. Geophys. Res., 77, 4602-4609 (1972).
3. Coles, W. A. and Kaufman, J. J., Solar wind velocity estimation from multi-station IPS, Radio Sci., 13, 591-597 (1978).
4. Coles, W. A., Harmon, J. K., Lazarus, A. J. and Sullivan, J. D., Comparison of 74-MHz interplanetary scintillation and IMP 7 observations of the solar wind during 1973, J. Geophys. Res., 83, 3337-3341 (1978).
5. Sime, D. G. and Rickett, B. J., The latitude and longitude structure of the solar wind speed from IPS observations, J. Geophys. Res., 83, 5757-5762 (1978).
6. Sime, D. G., Structure of the solar wind inferred from interplanetary scintillations, Ph.D. Thesis, University of California at San Diego, La Jolla, California (1976).
7. Rickett, B. J., Sime, D. G., Sheeley Jr., N. R., Crockett, W. R. and Tonsey, R., High latitude observations of solar wind streams and coronal holes, J. Geophys. Res., 81, 3845 (1976).
8. Coles, W. A., Rickett, B. J., Rumsey, V. H., Kaufman, J. J., Turley, D. G., Ananthakrishan, S., Armstrong, J. W., Harmon, J. K., Scott, S. L. and Sime, D. G., Solar cycle changes in the polar solar wind, Nature 286, 239-241 (1980).
9. Coles, W. A., and Rickett, B. J., IPS observations of the solar wind speed out of the ecliptic, J. Geophys. Res., 81, 4797-4799 (1976).
10. Kundu, M., Solar radio astronomy, Interscience Publishers, 18, (1965).

11. Hundhausen, A. J., Coronal expansion and solar wind, Springer-Verlag, 174-177 (1972).

12. Rickett, B. J., Disturbances in the solar wind from IPS measurements in August 1972, Solar Physics 43, 237-247 (1975).

13. De Young, D. S., and Hundhausen, A. J., Two dimensional simulation of flare-associated disturbances in the solar wind, J. Geophys. Res., 76, 2245-2253 (1971).

14. Rust et.al., Mass ejections, from Solar Flares - A monograph from Skylab Solar Workshop II, Colorado Associated University Press (1980).

APPENDIX Large H-α Flare - IPS Velocity Increase _ (100 km/s) Study

1972-1979 (All flares of A x B ≥ 1B and duration ≥ 120 min)

1972

Date	A x B	Duration	Location	IPS increase/no increase insufficient data
720517	2B	125	N16 E31	Insufficient
720528	2B	235	N09 E30	Yes
720711	1B	119	S08 W19	Yes
720802	2B	175	N13 E35	Yes
720804	3B	129	N14 E08	Insufficient
720807	3B	240	N16 W35	Yes
720921	1B	145	S07 E65	No
721215	2B	170	S06 E48	Insufficient

1973

Date	A x B	Duration	Location	IPS increase/no increase/ insufficient data
730411	1B	204	S08 W10	Yes (?)
730505	2B	207	S16 E18	Yes
730626	1B	125	S08 W27	Yes (?)
730729	3B	227	N14 E45	Yes (?)
730806	2B	141	N07 W05	Insufficient
730902	1B	141	S18 E55	Insufficient
730907	2B	170	S17 W47	Insufficient
731027	2B	130	N18 E54	Yes

1974

Date	A x B	Duration	Location	IPS Velocity Increase?
740416	1B	100	S14 W56	Yes
740513	3N	133	S11 W64	Yes
740526	1B	110	S16 W37	Yes (?)
740608	3N	130	S13 W64	Yes (?)
740623	3B	101	S13 W52	Yes (?)
740703	1B	101	S15 E08	Yes !
740704	2B	134	S16 W07	Yes (resolution)
740705	2B	147	S17 W26	
740707	1B	219	S16 W45	Yes
740913	2B	184	S15 E23	Yes
740918	1B	123	N12 W41	Yes
740919	2B	195	N08 W63	Yes
741013	1B	180	N13 W25	Yes (?)
74016	2B	103	N10 W63	Yes !

1975

750106	1B	105	N05 E20	Yes (?)
750619	1B	118	S09 W70	Yes (??)
751116	1B	134	S09 E47	Yes
751121	1B	155	S06 W23	Yes

1976

Date	A x B	Duration	Location	IPS Yes/No/Insufficient
760331	2N	207	S09 W09	Yes (?)
760430	2B	87	S09 W47	Yes !
760521	1N	117	S13 W24	Yes

1977

770416	2B	163	S21 E18	Yes (?)
770626	1B	103	S23 W18	No
770730	1B	105	N19 W42	Yes
770831	3B	55	N27 E85	Yes
770909	2B	150	N07 E87	Insufficient
770916	2B	275	N07 W21	Yes !
770919	3B	132	N08 W57	Yes !
771107	1N	179	S23 W45	Yes

1978

Date	A x B	Duration	Location	IPS Yes/No/Insufficient
780107	1N	131	S22 W71	Yes (?)
780203	3N	92	N33 W18	Yes
780207	1B	220	N14 E48	
780208	1B	126	N13 E41	
780209	1B	105	N25 W12	Yes (resolution)
780209	1B	229	N15 E29	
780209	1B	100	N15 E25	
780213	1B	141	N13 W24	Insufficient
780304	1B	120	N15 E45	Yes
780306	2B	166	N28 E22	Yes !
780408	3B	178	N20 W12	Yes
780413	1B	79	N20 W85	Yes
780428	3B	573	N23 E35	Yes !!
780429	2B	121	N20 E14	Yes
780501	2B	200	N21 W12	Yes (resolution)
780524	1B	115	N18 E42	Yes
780528	1B	100	N20 W13	Yes ! (resolution)
780531	4B	278	N21 W41	
780621	1B	103	S19 E66	Yes
780622	2B	357	N18 E16	Yes
780709	2B	222	N19 E70	
780709	2B	282	N17 E67	
780710	2B	101	N19 E58	
780710	1B	113	N19 E56	Yes (resolution)
780710	1B	184	N17 E54	
780711	2B	218	N18 E47	
780711	1B	119	N17 E41	
780729	2N	132	N23 E73	Yes
780830	1B	119	N19 E64	Yes (resolution)
780902	1B	99	S30 E37	
780907	1B	114	N35 E58	Yes
780915	1B	105	N36 E47	Yes (?)
780917	1B	112	N33 E30	
780923	3B	151	N35 W50	Yes !

1978 Continued

Date	A x B	Duration	Location	IPS Yes/No/Insufficient
780927	2B	156	N27 W20	Yes
781001	2B	140	S10 E55	Yes
781018	1B	178	S28 E32	Yes
781021	1B	96	S23 W67	Yes
781128	2B	163	N13 E47	Yes
781210	2N	107	S13 E29	
781211	2B	318	S16 W48	
781212	2B	93	S19 W73	
781212	2B	94	S19 W74	Yes (resolution)
781212	1B	124	S19 W67	
781213	2B	276	S14 E03	
781213	1B	138	S16 W73	
781227	3B	107	S13 E41	Insufficient (anti-solar)

1979

Date	A x B	Duration	Location	IPS Yes/No/Insufficient
790105	1B	95	S35 W17	Yes
790116	2N	104	N20 W54	Yes (?)
790201	3B	83	S21 E90	Yes
790208	1B	102	S18 E14	Yes (resolution)
790208	1B	92	N17 W63	
790210	1B	201	N13 W24	Yes
790216	3B	95	N16 E59	Yes
790217	1B	95	N18 E02	Yes (resolution)
790217	1B	108	N17 W02	
790218	2B	105	N16 E16	
790218	2B	93	N17 W13	
790219	1B	140	N19 W28	
790219	2B	121	N20 E02	
790220	2B	99	N01 W33	Yes (resolution)
790220	2B	145	N20 W25	
790305	1B	155	N12 E25	Insufficient (anti-solar)
790311	1B	114	S14 W05	Insufficient (anti-solar)
790316	1B	140	N19 W20	Yes
790322	2B	101	N07 W28	Insufficient (anti-solar)
790326	1B	104	N09 W68	Yes !
790329	3B	66	S30 E56	Yes (resolution)
790330	2B	61	S25 E31	
790403	1B	140	S26 W14	Yes ! Only flares of $\geq$ 1B, 120 min
790417	1B	204	N28 W12	Yes
790426	1B	139	N11 E39	No
790503	1B	132	S26 E47	Yes
790605	3B	228	N18 E14	Yes !
790610	3B	142	N21 W45	Insufficient
790704	2B	137	N13 E35	Yes !
790709	1B	139	S29 E11	Yes
790721	1B	185	N14 W48	No
790814	1B	300	S22 E73	Yes (coronal transient)
790820	1B	121	S16 E14	Yes

1979 Continued

Date	A x B	Duration	Location	IPS Yes/No/Insufficient
790823	1B	125	N07 E29	No
790826	2B	307	N05 W12	Yes
790831	1B	232	N13 E59	Insufficient
790919	1B	289	N05 E36	Insufficient
791007	1B	146	N15 E33	Insufficient
791026	1B	124	S18 E05	Insufficient
791109	1B	176	S20 W59	Insufficient
791110	1B	127	S19 W68	Yes (?)
791115	2B	151	N29 W38	No

Table 1.1: Flares $\geq$ 2B and Duration $\geq$ 120 min

Year	# Flares $\geq$ 2B and $\geq$ 120 min	# Assoc. IPS Vel. Increases	# Not Enough IPS Data	# Definite No Increase in IPS	(# Sources hit)/ (# Avail. Sources)
1972*	6	3	3	0	3/3
1973	4	1	1	2	1/1
1974	3	3	0	0	2/4
1975	0	0	0	0	-
1976	0	0	0	0	-
1977	4	3	1	0	2/3
1978	13	11	1	1	3/3
1979	6	5	1	0	2/2
	36	24	7	3	2/3

Table 1.2: Flares = 1B and Duration $\geq$ 120 min

Year	# Flares = 1B and $\geq$ 120 min	# Assoc. IPS Vel. Increases	# Not Enough IPS Data	# Definite No Increase in IPS	(# Sources hit)/ (# Avail. Sources)
1972*	2	1	1	0	4/5
1973	3	1	2	0	2/3
1974	3	2	1	0	2/2
1975	2	0	2	0	-
1976	0	0	0	0	-
1977	0	0	0	0	2/3
1978	5	3	1	1	2/3
1979	17	10	3	4	2/4
	32	17	10	5	2/3

*Starting April

Table 1.3: Flares ≥ 1B and Duration between 60-120 min

Year	# Flares ≥ 1B and duration 60-120 min.	# Assoc. IPS Vel. Increases	# Not Enough IPS Data	# Definite No Increase in IPS	(# Sources hit)/ (# Avail. Sources)
1972*	25	7	14	4	1/2
1973	13	7	5	1	1/2
1974	11	5	2	4	2/2
1975	8	2	2	4	2/3
1976	4	4	0	0	1/3
1977	7	1	2	4	1/3
1978	23	12	6	5	1/2
1979	44	14	20	10	2/2
	135	52	51	32	1/2

*Starting April

Table 3.1. To show that flares occurred on same active region of sun. (Also indicates presence or absence of type II & IV radio bursts concurrent with the flare.)

Date (1978) (magnitude)	Position on Sun	Rotation #	Type II or IV
March 06 (2B)	N28 E22	1.000	II only
April 13 (1B)	N20 W85	2.096	None
April 28 (3B)	N23 E35	2.979	II, IV
May 31 (4B)	N21 W41	3.978	II, IV
June 22 (2B)	N18 E16	4.944	II, IV
July 09 (2B)	N19 E70	5.717	None

Table 3.2. Response of the earth's magnetic field to the flares (K_p index changes)

Flare	Angular displacement (equatorial plan)	Flare duration (min)	+Geomagnetic disturbance duration (hrs)	Average speed toward earth (from SSC onset time
March 06	E22°	166	12	840
April 13	W85°	79	-	-
April 28	E35°	573	108*	927
May 31	W41°	278	21	868
June 22	E16°	357	39	580?
July 09	E70°	222	-	-

*Several flares during April 28-May 02.

+Approximately the time taken for the K_p index to fall to 1/2 its peak value.

Table 3.3. IPS velocity response to the flares

Flare Date (Day Number)	IPS velocity (V_{mid}) before & after flare response km/s (day #)	km/s (day #)	Angular displacement of flare normal & sub-scattering pt	Radio Source
March 06 (65)	434 (65)	830 (66)	E17°	3C48
April 13 (103)	517 (103)	678 (104)	E28°	3C459
April 28 (118)	311 (119)	690 (120)	W04°	3C161
May 31 (151)	365 (152)	764 (153)	E21°	3C459
June 22 (173)	321 (175)	656 (176)	E15°	3C237
July 09 (190)	279 (190)	625 (192)	W23°	3C237
Avg:	371	707		

Table 3.4. Summary of observed and average speeds from IPS and K_p

Flare	IPS measured velocity (km/s) (V_{mid}, V_{pk})	Avg. velocity from IPS (km/s) (min, max)	Distance to S.S. point (AU)	Avg. velocity from K_p data (km/s)
March 06	830 814 (3C48)	908 2802	0.79	840
April 13	678 764 (3C459)	594 1681	0.54	-
April 28	690 635 (3C161)	1000 3017	0.88	927
May 31	764 787 (3C459)	771 1411	1.00	868
June 22	656 588 (3C237)	561 885	0.90	580?
July 09	625 612 (3C237)	513 2948	0.73	-

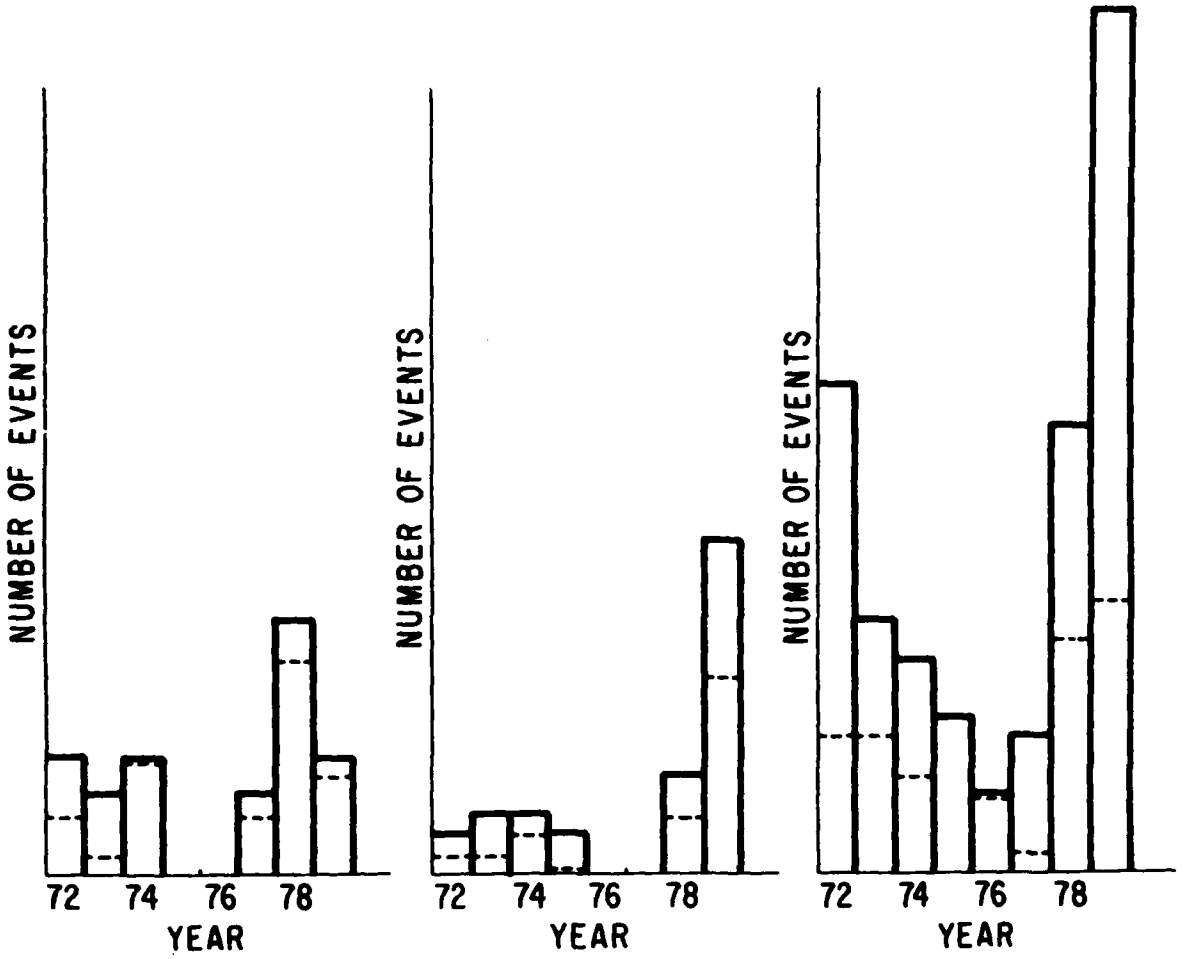

Figure 1.1 - Hα flare - IPS velocity increase statistics. Flares grouped according to area, brightness, and duration. The solid lines indicate the number of flares in each category for a given year (1972-1979). The broken line indicates the number of associated IPS velocity increases.

1.1(a) - area x brightness $\geq$ 2B and duration $\geq$ 120 min.

1.1(b) - area x brightness = 1B and duration $\geq$ 120 min.

1.1(c) - area brightness $\geq$ 1B and duration 60 - 120 min.

*Starting April 1972

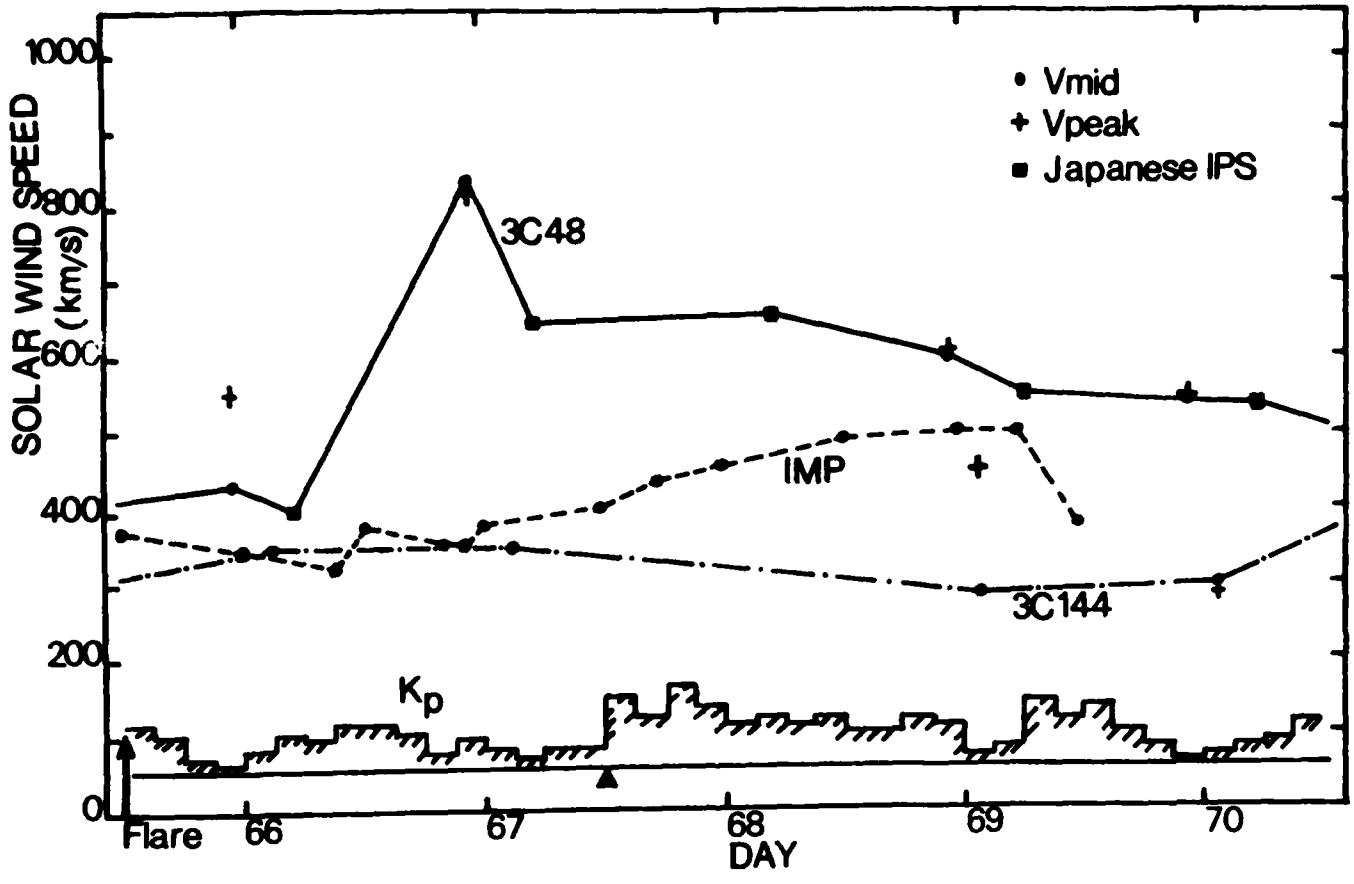

Figure 2.1 - Solar wind response to the flare of March 6, 1978. Solid lines indicate the daily IPS observations of radio sources 3C 48 and 3C 144. Broken lines indicate 3 hour averages of solar wind speed observed by earth orbiting spacecraft IMP 7 and 8. Histogram at bottom is the K_p index (3 hour averages).

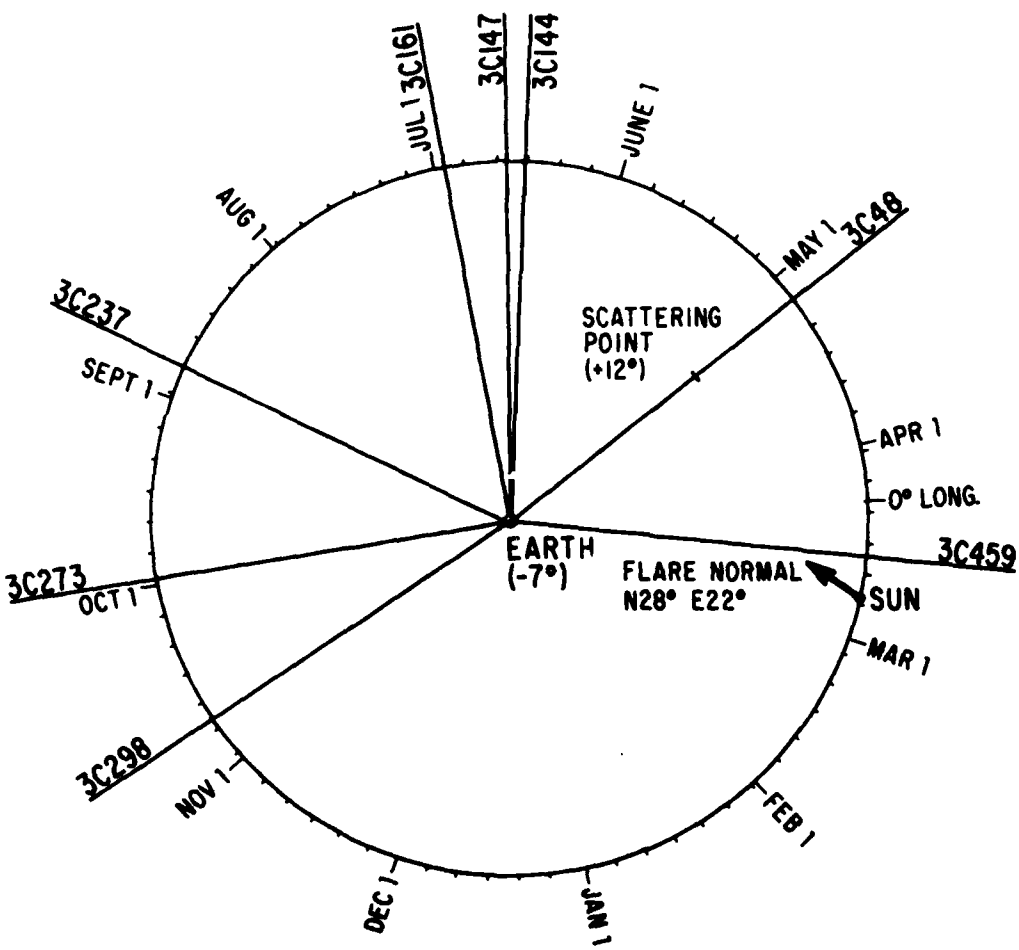

Figure 2.2 - Ecliptic projection of the radio source positions, earth, sun and the flare normals for the events of March 6, 1978.

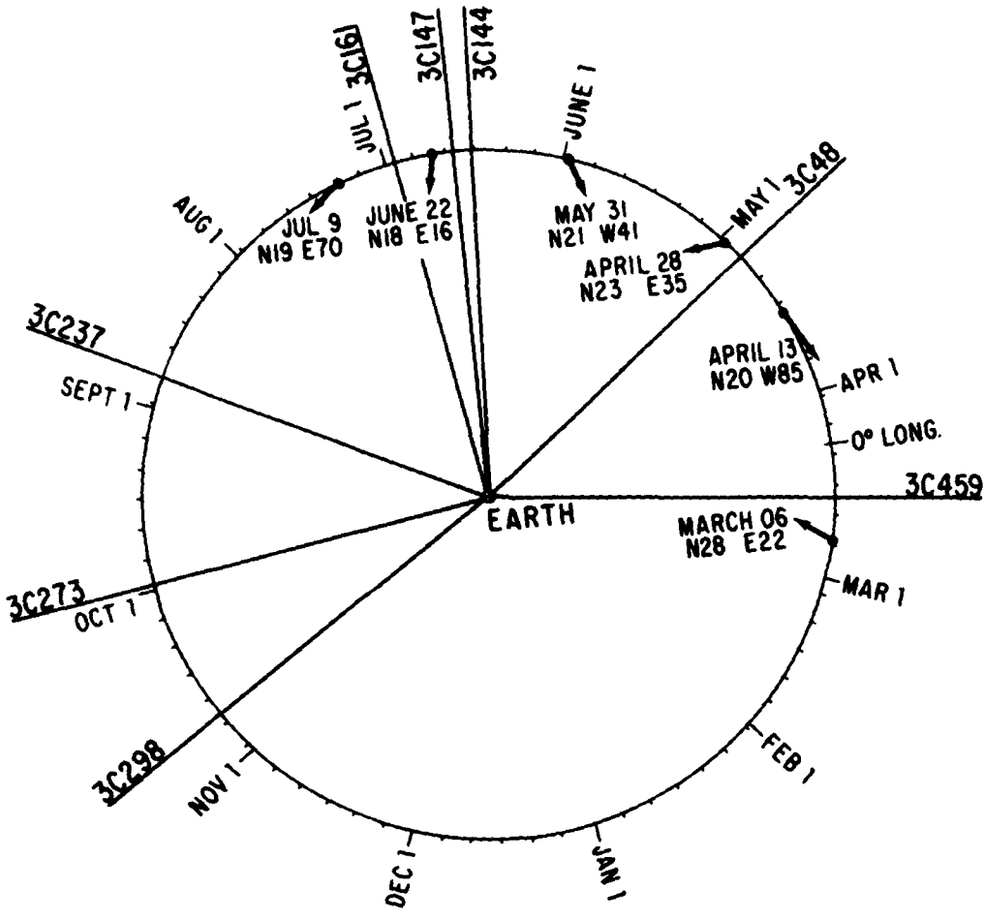

Figure 3.1 - Ecliptic projection of the radio source positions, earth, sun and the flare normals for the events of March 6, April 13, April 28, May 31, June 22, July 9.

IPS SOLAR WIND VELOCITIES FROM NEW SOURCES

B. V. Jackson

Department of Electrical Engineering and Computer Sciences

University of California, San Diego

La Jolla, California 92093

Abstract

In 1979 we began a systematic search and analysis of solar wind velocities from radio sources other than the original 8 observed by UCSD since 1972. Each new source was calibrated by UCSD's 74 MHz system. In May 1980 ten new sources were added to the list of those regularly analyzed for solar wind velocities. We expect these sources to give better spatial resolution for observations during times of enhanced IPS. They also define the size of equipment needed to observe large numbers of sources enabling the resolution of solar velocity structures on a daily basis.

The UCSD 73.8 MHz arrays have been used to observe interplanetary scintillation (IPS) from 8 sources daily since 1972. These sources, among the strongest scintillators at this frequency continue to give much valuable information about the scintillation process - the nature of the solar wind in the ecliptic plane and above the poles of the sun throughout the solar cycle. However, higher spatial resolution obtained by observing more sources would allow much more information to be gathered on a daily basis. With many sources we would no longer have to average for one or more solar rotations, but could make maps of the solar wind velocity structure on a daily basis and study its evolution. In addition, coronal transients could be studied in more detail as they propagate through the interplanetary medium in studies similar to that of Vlasov (1978). In the past, a few additional sources observed by us occasionally showed scintillation, but until FY '79-80 no concerted effort was made to study and analyze solar wind data from these weaker sources. In the summer of 1979, we began a search of the strongest scintillating sources in the Readhead and Hewish (1974) 81.5 MHz catalogue. This study determined how well the present equipment could be used to obtain solar wind speeds from these sources.

Each new source observed was given a daily IPS performance rating similar to the ratings reported to Solar Geophysical Data (1973-80). Figure 1 presents an average rating value for the time period the new and old sources were observed versus the log of the relative gain for each source using our equipment. Several sources were measured at different times corresponding to different relative gains. In general, these sources fell along a straight line parallel to that in Figure 1. It is interesting to note that to the extent that the sources plotted in Figure 1 fall along a straight line, our rating system is linear relative to the log of the scintillation flux squared as determined by Readhead and Hewish (1974). Twenty-five sources observed and rated by this technique and calibrated by scintillation flux at 81.5 MHz are displayed in ecliptic

coordinates in Figure 2. One source, 3C 283, was too far south (δ = -22°) to be included in the Readhead and Hewish (1974) catalogue, but gives strong and reliable scintillations on our equipment.

Having calibrated our instrument with respect to a few of the 1500 sources observed by Readhead and Hewish, we can now determine how much bigger arrays would be needed in order to observe some of the weaker sources with the same quality as the original 8. We find from source counts in the Readhead and Hewish catalogue that doubling the area of our telescopes would allow $\sim$25 sources to be observed on a regular basis. If our equipment were expanded to 4 times its present area, we would be able to observe nearly 200 sources with the same quality as the original 8. The numbers in the catalog are close to those expected for uniform Euclidian geometry but not all regions of the sky have equal numbers of scintillators. Especially void of strong sources is the region in the Milky Way near the Galactic center; the sun crosses this region in December. In addition, the sun is the farthest south in December and sources east or south of the sun will be most difficult to observe from our northern latitude during this time period.

In April 1980 we began regular observations of 10 additional sources with our present equipment. Table 1 presents the observing times for these sources; these times are compared with the observing times for the original 8 sources. Although some of the observing times of the additional 8 sources were shortened or changed slightly to make room for the additional sources, no degradation from the original source signal was noted following these changes. On days of enhanced turbulence, nearly all the sources scintillate well enough to have their velocities reported to the Space Environment Forecast Center in Boulder.

References

Readhead, A. C. S., and Hewish, A.: 1974, Mem. R. Astr. Soc. 78, 1.

Vlasov, V. I.: 1978, Soviet Journal of Physics 53, 1.

Table 1

SOURCE	Local Sidereal Time of Observation After April 1980	Before April 1980
3C144-	0305 - 0335	0305 - 0335
3C138	0335 - 0420	
3C147	0420 - 0510	0421 - 0513
3C144	0510 - 0524	0513 - 0527
144 Scan	0524 - 0531	0527 - 0531
3C144	0531 - 0554	0531 - 0553
144 Scan	0554 - 0620	0553 - 0620
3C161	0620 - 0735	0620 - 0735
3C196	0735 - 0805	
3C144+	0805 - 0835	0805 - 0836
3C216	0835 - 0926	
3C222	0926 - 1017	
3C237	1017 - 1119	0958 - 1108
CAL	1119 - 1126	
3C273	1126 - 1230	1154 - 1319
3C283	1230 - 1330	
3C295	1330 - 1425	
3C298	1425 - 1626	1325 - 1516
CAL	1626 - 1632	
No Data	1632 - 1700	
3C368	1700 - 1830	
1st Cygnus Scan	1830 - 1925	
CAL	1925 - 1930	
2nd Cygnus Scan	1930 - 2040	
3C409	2040 - 2154	
3C446	2154 - 2300	
3C459	2300 - 2440	2131 - 2434
CAL	2440 - 2446	
3C48	2446 - 2623	2434 - 2659
3C123	2623 - 2659	
No Data	2659 - 0305	

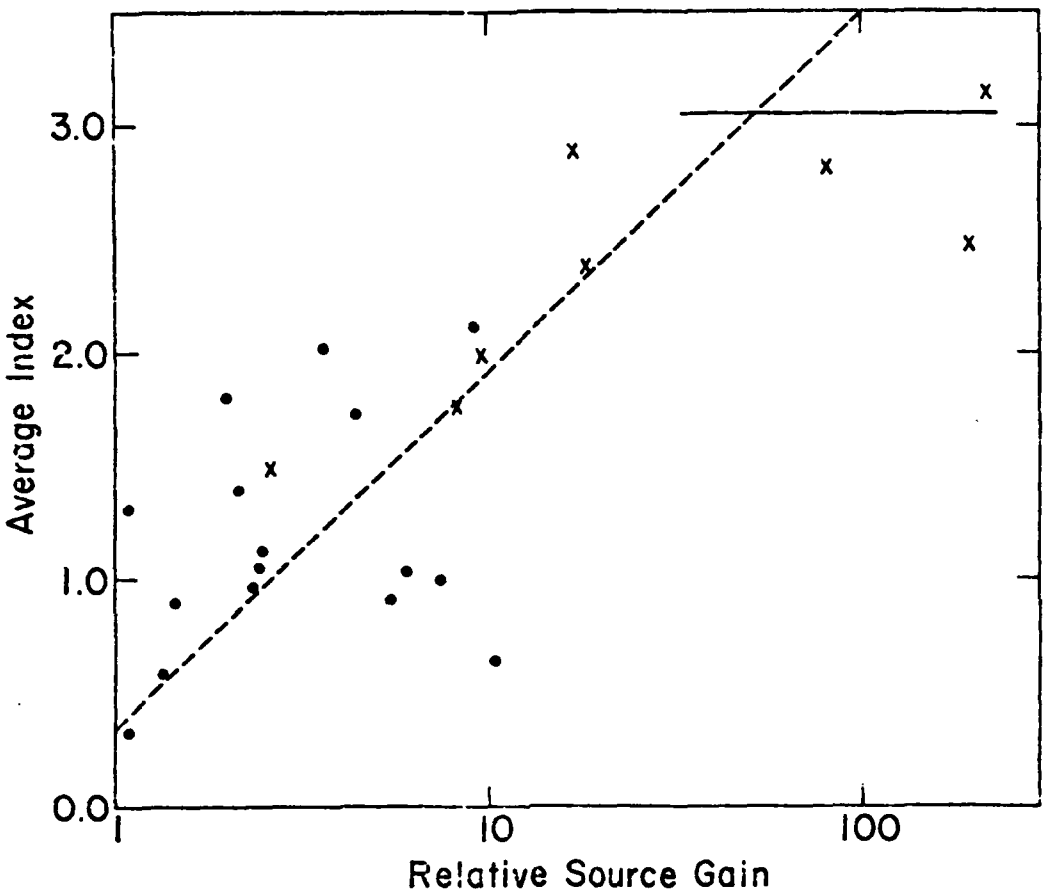

Figure 1 - Source performance for original 8 sources (x) and new sources (•). The average index is the daily source rating (0-5) of each source divided by the number of days the source was observed. Relative Source Gain = $(\Delta S \cdot GF \cdot EF_{\bullet})^2 (OT)^{1/2}$ where ΔS is the source scintillation flux strength at 81.5 MHz from Readhead and Hewish (1974), GF the relative gain of the beams used to observe the source, EF the relative source scintillation strength according to source elongation assuming the source is like 3C 144 and OT the length of observation. The dashed line is a least squares line fit to the points. The coefficient of determination of this line is $R^2 = 0.58$. The horizontal line represents the average index of 3C 283 and allows a determination of S for this source.

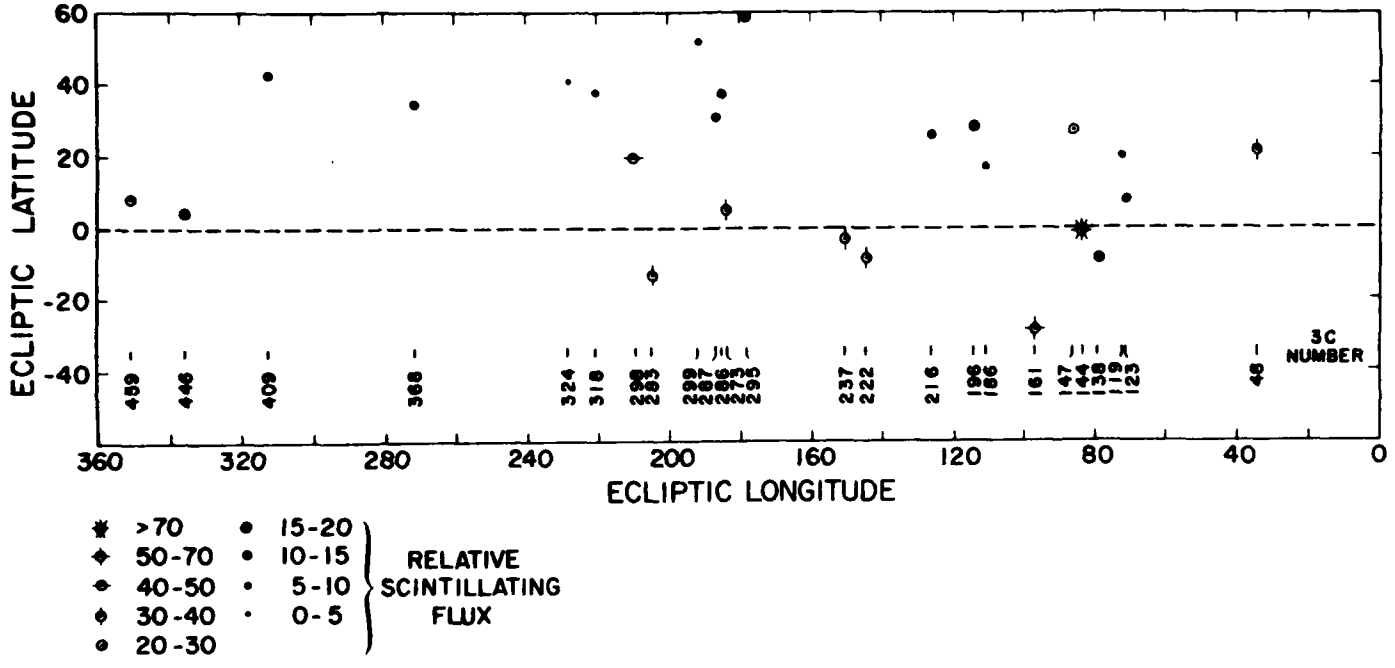

Figure 2 - Relative strength of sources and their positions in the sky. Scintillating flux strength is normalized to the Readhead and Hewish (1974) 81.5 MHz source fluxes by the plot in Figure 1. Relative individual source scintillation strengths at 74 MHz are determined by the change in scintillating flux strength needed to shift the source to the least squares line fit to all points.

END

DATE
FILMED
1-82

DTIC